



## M Shell Fluorescence Parameters of Pt, Au and Tl Compounds with Oxygen and Bromide

Nuray Kup AYLIKCI<sup>1,\*</sup>, Volkan AYLIKCI<sup>2</sup>, Engin TIRASOGLU<sup>3</sup>, Tolga DEPCI<sup>4</sup>

<sup>1</sup>Iskenderun Technical University, Faculty of Natural Sciences and Engineering, Energy Systems Engineering, Hatay, Turkey

*nuray.aylikci@iste.edu.tr, ORCID: 0000-0002-2276-5421*

<sup>2</sup>Iskenderun Technical University, Faculty of Natural Sciences and Engineering, Metallurgical and Material Engineering, Hatay, Turkey

*volkan.aylikci@iste.edu.tr, ORCID: 0000-0002-5747-0754*

<sup>3</sup>Karadeniz Technical University, Faculty of Science, Department of Physics, Trabzon, Turkey  
*engint@ktu.edu.tr, ORCID: 0000-0001-7953-5638*

<sup>4</sup>Iskenderun Technical University, Faculty of Natural Sciences and Engineering, Department of Engineering Sciences, Hatay, Turkey

*tolga.depci@iste.edu.tr, ORCID: 0000-0001-9562-8068*

### Abstract

In this study,  $M_{\beta\alpha}$  X-ray production cross-sections and average M-shell fluorescence yields were determined by using EDXRF at 5.96 keV for Pt, Au and Tl compounds. The photo-peak areas were used for the measurement of M X-ray production cross-sections and also other parameters. The obtained values were compared with the theoretical values in the literature to explain the changes in parameters. It was obtained that the changes were resulted from the electronegativity differences between Pt, Br and O in Pt compounds and Au, Br and O in Au compounds. As for Tl compounds, it was obtained different results and attributed to both of the charge transfer from one element to another and polarizability mechanisms of Tl.

**Keywords:**  $M_{\beta\alpha}$  X-ray production cross-section, Average M-shell fluorescence yield, EDXRF

\* Corresponding Author

Received: 25 January 2019

Accepted: 16 December 2019

## Oksijen ve Bromlu Pt, Au and Tl Bileşiklerinin M Kabuğu Floresans Parametreleri

### Öz

Bu çalışmada,  $M_{\beta\alpha}$  X-ışını üretim tesir kesitleri ve ortalama M kabuğu flüoresans verimleri 5.96 keV enerjide, EDXRF yöntemi kullanılarak Pt, Au ve Tl bileşikleri için belirlenmiştir. Foto-piklerin altında kalan alanlar M X-ışını üretim tesir kesitlerinin ve aynı zamanda diğer parametrelerin ölçülmesinde kullanılmıştır. Elde edilen değerler, parametrelerdeki değişimi açıklamak için literatürdeki teorik değerlerle kıyaslanmıştır. Değişimlerin Pt bileşiklerinde Pt, Br ve O arasındaki, Au bileşiklerinde ise Au, Br ve O elementleri arasındaki elektronegativite farkından kaynaklandığı belirtilmiştir. Tl bileşiklerinde ise değişimler hem bir elementten diğerine yük transferi hem de Tl elementinin polarize olabilmesi mekanizmalarına atfedilmiştir.

*Anahtar Kelimeler:*  $M_{\beta\alpha}$  X-ışını üretim tesiri kesiti, Ortalama M kabuğu flüoresans verimi, EDXRF

### 1. Introduction

The fundamental X-ray fluorescence parameters are sensitive tools for the investigations of complex shell structures of any atom. Even small changes in electronic structures of any atom affect the measured parameters. Also, these measured or calculated parameters constitute an essential data for developing more sensitive devices related with spectroscopic measurements. An X-ray transition exposes when a hole is created at the innermost shell of any atom. The created hole will be filled by an outermost shell electron resulting in X-ray transition [1].

The compounds that are studied in the concept of this paper have many applications in different areas. For example, Pt and its oxidized compound is an essential material as an electrode owing to the high capability of oxygen reduction reaction in fuel cells. Especially,  $PtO_2$  form can be originate on the surface of Pt in oxygen rich conditions or can be originate in the case of potential-applied interfaces. The case of second one is used for proton-exchange membrane fuel cell applications and fuel cells are important materials for the production of clean energy [2]. In the literature, it was emphasized that

Pt-based cancer drugs such as PtBr<sub>2</sub> had a productive radio and photosensitizer property for clinical therapy. And the effective cancer drug could be produced if it was contained both Pt and Br element [3]. It is known that Au element has the highest electro-conductivity and is the most resistant element to oxidization in oxygen rich chemical environment. Au element can be oxidized under several conditions such as 1000 atm pressure or highly reactive chemical environments and the oxidized form of Au is usually utilized as a catalyst [4]. Au complexes such as AuBr<sub>3</sub> are an effective material to increase the work function of graphene [5]. Also, it is known that Tl element is used for semiconductor detectors, but its oxidized forms can be used in different application of any material such as high temperature super conductors or producing of glasses which have high refractive index. The different application area of these chemical compounds is promoted us to investigate the M-shell X-ray fluorescence parameters at 5.96 keV not only for elements but also the chemical compounds. The energy dispersive X-ray fluorescence method is an easy, practical and non-destructive analyzing method to investigate the shell structure of compounds by using the changes in X-ray transitions.

It is generally known that each atom has a set of separate energy levels. Considering the composition of N free atoms, the distribution of the quantum states of this system is the same as the repeating of one atom N times. The wave functions of the outer electrons of neighboring atoms begin to overlap. These outer electrons of one atom begin to feel the potential of the nucleus which is belong to the neighboring atom. When a vacancy is created in an inner shell, the created vacancy will be filled by radiative or radiationless transitions. For instance, the transitions from the outer shells or valence shells will be more affected transitions for any chemical compounds since the change in the electron density of any states leads to the alteration of binding energy of outer shell electrons and so the radiative and radiationless transition rates. In this case, the increment in the screening effect of valence electrons (or transferring of valence electrons from one element to another) decrease the binding energy of outer shell electrons because of the fell less nuclear charge compared to the pure state. It is known that the total probability of X-ray transitions (include radiative and radiationless transitions) are equal to 1 and one quantity will show increment tendency where the other is decreased.

It is known that M X-ray fluorescence parameters are essential for many applications apart from the atomic physics studies including the surface chemical analysis, dosimetric computations for health physics, cancer therapy and industrial irradiation processing [6]. In the literature, M shell fluorescence parameters were investigated by using different methods or different calculation procedures at different photon energies. The experimental determination on fluorescence parameters by using Mn K X-ray photon energy, total M X-ray cross-sections for Yb, Lu, Ta, W, Re, Au, Hg, Tl, Pb, Br, Th and U elements were determined at 5.96 keV [7]. Also, by using  $^{55}\text{Fe}$  radioactive source, X-ray production cross-sections and average M shell fluorescence yields were measured for Lu, Hf, Ta, Ir, Pt, Au, Pb, Bi, Th and U [8]. Average M shell fluorescence yields were determined for Pt, Au and Pb elements at different photon energies changing in the range  $5.47 \leq E \leq 9.36$  keV and from the fluorescence yield measurements, total M shell photoionization cross-section values were deduced [9]. The probability of the group of M X-ray production was investigated by using different photon energies for elements  $67 \leq Z \leq 92$ . The obtained parameters were used for the testing the tabulated theoretical models by using independent particle model where the Coulomb interactions were ignored between one electron with another in the same atom. It was emphasized that the calculations for M shell Coster-Kronig transitions were achieved by incorporating many particle model [10]. Using the synchrotron radiation source with linearly polarized, M sub-shell X-ray emission cross-sections were measured for Pt, Au, Hg, Pb, Th and U at 8 and 10 keV energies. The measured data were compared with the obtained theoretical ones where Dirac-Hartree-Slater and Dirac-Fock approximations were used [11]. Differential and total M shell X-ray production cross-sections of some selected elements from Au element to U were determined at different angles by using Si(Li) detector. The measured values were compared with the other values which were semi-empirically fitted. It was emphasized that the differential M shell X-ray production cross-sections were decreased by increasing emission angle and showed an anisotropic spatial distribution [12]. Using ECPSSR theory, M shell X-ray production cross-sections were determined both empirically and semi-empirically by proton energy between 0.1 and 4.0 MeV for elements from Hf to Th. In the study, the most reliable values were achieved by globally fitting procedure and from the fitted equation new values were obtained [13].

It can be achieved more studies about the M shell calculations or measurements using different irradiation source, different elements, different angles and different energy ranges [14-23]. Due to the complexity structure of M shell, the parameters were determined for pure elements and different energy ranges. But, there are not much more studies about the M shell fluorescence parameter calculations according to the different valence shell electronic distributions. Similar studies can be found such as chemical shift in X-ray emission lines, electronic wave function and binding effect and multiple ionization effects. From the wave-length dispersive X-ray fluorescence measurements, positive and negative shifts in L X-ray emission lines were recorded for Ag, Cd and Sn elements in different chemical compounds. And also, from the theoretical calculations of effective charges, it was found that the calculated values were linear dependent with the chemical shifts. The obtained chemical shifts values were correlated with the bond length of compounds, relative line widths, effective charge, electronegativity, number of ligands and Coster-Kronig transition process [24]. The discrepancies in the calculation of parameters related with M subshell ionization of gold were attributed to the inadequate description of electron binding effect at the lowest irradiation energies where the molecular approach was important [25]. And finally, multiple ionization effects were studied for M X-ray emission lines induced by Ar<sup>12+</sup> ions. The obtained values of W were compared with the calculated values of PWBA and ECPSSR theories and two extreme assumptions were considered which called as single ionization and full ionization [26].

Energy dispersive X-ray fluorescence analysis is a non-destructive and practical way and the measurements can be repeated many times to shrink the statistical errors. Since the complexity structure of M shell, there is less study about the measurement of M shell fluorescence parameters of high atomic number elements using energy dispersive X-ray fluorescence. Also, these obtained data is important for understanding of atomic shell structure of any atom. Namely, a large number of data allows to the improvement new updated theoretical models and also the development of new spectroscopic devices. In this study, average M shell fluorescence yields and M X-ray production cross-section values were measured for Pt, Au and Tl elements in different oxidized and bromide compounds. The obtained data in this study will shed light for the development of new theoretical models to understand the complexity structure of M subshell and required for

different application areas such as radiation shielding, radiation attenuation and dosimetric calculations.

## 2. Materials and Methods

The thin films examined in this study were prepared by distributing powder samples as homogeneous as possible to  $1.44 \text{ cm}^2$  area on the Mylar film. The prepared thin films were placed in the experimental geometry to be stimulated by radioactive source and to count the characteristic X-rays that occurred. The geometry of experimental set-up and the calibration process are the same as in our previous studies [1, 27–29] and the produced thin films were irradiated with 5.96 keV energy X-rays released from a filtered  $^{55}\text{Fe}$  radioactive annular source which has 50 mCi activity. For each prepared sample, the measurement time is selected as 5000 seconds to obtain statistical sensitivity. The energy of released X-rays was determined to be larger than M sub-shell absorption edge. The emitted X-rays from the irradiated thin films were counted by an Ultra-LEGe detector whose FWHM was 150 eV at 5.9 keV. The obtained M shell spectra were analyzed by using Origin Company software program using least square fitting module. The photo-peak areas were used to determine average M X-ray production cross-sections and so average M shell fluorescence yields of elements in studied chemical compounds. The plotted peaks for  $\text{PtO}_2$ ,  $\text{AuBr}_3$  and  $\text{TlO}_2$  compounds were shown as Fig. 1, 2 and 3 respectively.

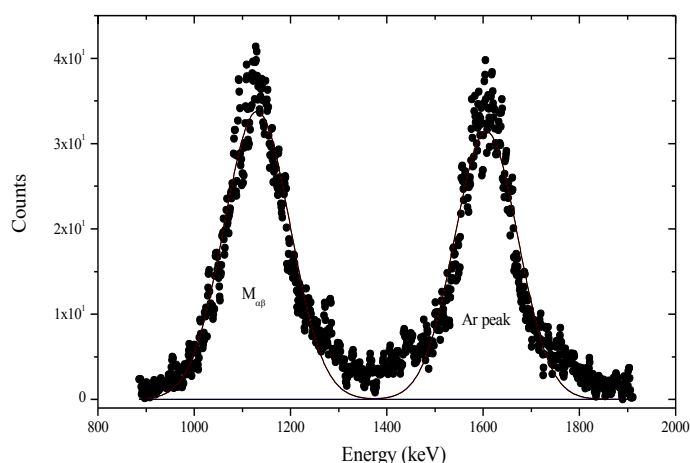


Figure 1. M X-ray peaks for  $\text{PtO}_2$  compound

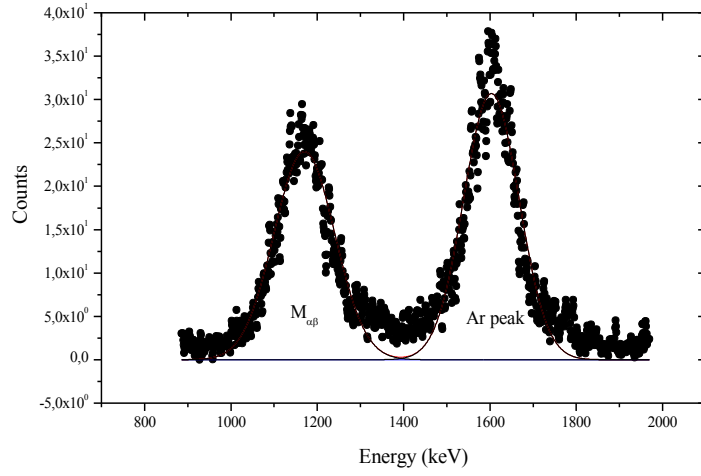


Figure 2. M X-ray peaks for AuBr<sub>3</sub> compound

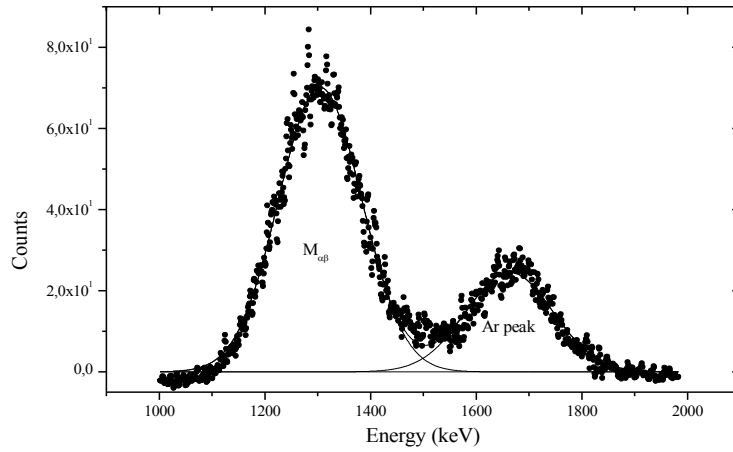


Figure 3. M X-ray peaks for TiO<sub>2</sub> compound

The photo-peak areas were used for the calculation of M X-ray production cross-section values as written below.

$$\sigma_{M_{\alpha\beta}}^X = \frac{M}{N} \frac{N_{M_{\alpha\beta}}^X}{I_0 G \varepsilon_{M_{\alpha\beta}}^X \beta_{M_{\alpha\beta}}^X m} \quad (1)$$

Total photo-peak area is denoted as  $N_{M_{\alpha\beta}}^X$  (see in Figs. 1–3), the product of the intensity of radiation impinging on sample and the geometry factor is symbolized as  $I_0 G$  and finally the detector efficiency, self-absorption correction factor, the mass thickness

of the specimens are demonstrated as  $\varepsilon_{M_{\alpha\beta}^x}$ ,  $\beta_{M_{\alpha\beta}^x}$  and  $m$  respectively.  $M$  denotes the molecular weight and  $N$  is the Avogadro constant. The detailed information about the detector geometry and the detector efficiency were explained as in our previous study [1]. The self-absorption correction factor was determined by using the total mass absorption coefficients of studied compounds and the angles of incident and emitted radiation. The relation for the determination of self-absorption correction factor is written as below;

$$\beta_{M^x} = \frac{1 - \exp\left[-\left(\frac{\mu_p}{\cos\theta_1} + \frac{\mu_e}{\cos\theta_2}\right)m\right]}{\left(\frac{\mu_p}{\cos\theta_1} + \frac{\mu_e}{\cos\theta_2}\right)m} \quad (2)$$

The quantities  $\mu_p$  and  $\mu_e$  are determined by using XCOM [30] which shows the total mass absorption for target material (or studied compounds) at the irradiated photon energy and at the studied emission energy [31] from the material. The angles  $\theta_1$  and  $\theta_2$  that cosine values are used in Eq. (2), shows the incident and emitted photon angles respectively. These values are determined according to the normal of target surface. In this study, the incident angle of the photons from the radioactive source is set as  $45^\circ$  and so the emission angle for X-ray photons from the specimens will be  $0^\circ$ .

It is known that the probability of the production X-rays for studied electronic shells or sub-shells can be determined by measuring the X-ray production cross-section values. In our detector system, all X-ray transitions from upper shells to M shell cannot be resolved since it has low resolution value to separate  $M_\alpha$  and  $M_\beta$  X-rays. And so the average M shell fluorescence yields can be determined by using the ratio of the total M shell X-ray production cross-section,  $\sigma_{M_{\alpha\beta}}^X$  to the M shell photoionization cross-section,  $\sigma_M^P$  at 5.96 keV [32].

$$\bar{\omega}_M = \frac{\sigma_{M_{\alpha\beta}}^X}{\sigma_M^P} \quad (3)$$

### 3. Result and Discussion

The electronic distribution is  $[\text{Xe}]4f^{14}5d^96s^1$  for Pt,  $[\text{Xe}]4f^{14}5d^{10}6s^1$  for Au and finally,  $[\text{Xe}]4f^{14}5d^{10}6s^26p^1$  for Tl.  $M_{\alpha}$  and  $M_{\beta}$  X-ray lines are emitted from N sub- shells by the absorption of photons in  $M_{IV}$  and  $M_V$  levels and the valence states are located in N shells for studied elements in different compounds. To investigate the valence shell structure by using X-ray transitions, the empirical M shell X-ray production cross-section and average M shell fluorescence yields are measured and demonstrated as Tables 1 and 2 respectively for Pt, Au and Tl compounds with calculated values in other studies.

Table 1.  $M_{\alpha\beta}$  X-ray production cross-sections of Pt, Au and Tl compounds

Specimens	$\sigma_{M_{\alpha\beta}}$			$\sigma_M^x$			
	Exp.	Theoretical [33]	Exp. [34]	Fitted [34]	Exp. [9]	Exp. [8]	Fitted [35]
Pt	7.008±0.357	6.41	8.23±0.34	8.538	8.454±0.70	9.24±0.74	8.65
PtO <sub>2</sub>	8.811±0.449	--	--	--	--	--	--
PtBr <sub>2</sub>	8.461±0.432	--	--	--	--	--	--
Au	7.731±0.394	7.28	9.38±0.49	9.211	9.226±0.70	10.12±0.81	9.51
Au <sub>2</sub> O <sub>3</sub>	9.856±0.503	--	--	--	--	--	--
AuBr <sub>3</sub>	9.626±0.491	--	--	--	--	--	--
Tl	--	8.67	--	--	--	--	11.38
TlO <sub>2</sub>	10.376±0.529	--	--	--	--	--	--
Tl <sub>2</sub> O <sub>3</sub>	10.588±0.540	--	--	--	--	--	--
TlNO <sub>3</sub>	10.108±0.516	--	--	--	--	--	--
Tl <sub>2</sub> CO <sub>3</sub>	10.277±0.524	--	--	--	--	--	--

According to Table 1, it will be seen that  $M_{\alpha\beta}$  X-ray production cross-sections are different from the elemental and other values in the literature [8, 9, 33–35]. But it must be noted that  $M_{\alpha\beta}$  X-ray production cross-section values in the literature are cited as Ref. [33] and other values denote the total M shell production cross-section values where all transitions from N shell to M shell are considered. The measured  $M_{\alpha\beta}$  X-ray production cross-section values 37% and 32% higher for PtO<sub>2</sub>, PtBr<sub>2</sub> compounds, 35% and 32% higher for Au<sub>2</sub>O<sub>3</sub>, AuBr<sub>3</sub> compounds, finally 19%, 22%, 16% and 18% higher for TlO<sub>2</sub>, Tl<sub>2</sub>O<sub>3</sub>, TlNO<sub>3</sub>, Tl<sub>2</sub>CO<sub>3</sub> compounds respectively. Since the studies which referenced as [8, 9, 34, 35] considered all M shell X-ray transitions, the comparisons will be made by using Ref. [33] where the calculations are performed by using only  $M_{\alpha}$  and  $M_{\beta}$  transitions. The reason of these differences can be explained by using different notions such as bond energy, electronegativity, screening effect or effective nuclear charge.

Table 2. Average M-shell fluorescence yields of Pt, Au and Tl compounds

Specimens	$\omega_{M,5}$			
	Experiment	Fitted [35]	Theoretical [36]	Theoretical [37]
Pt	0.0211±0.0011	0.0257	0.0252	0.0264
PtO <sub>2</sub>	0.0265±0.0014	--	--	--
PtBr <sub>2</sub>	0.0254±0.0013	--	--	--
Au	0.0229±0.0012	0.0278	0.0267	0.0276
Au <sub>2</sub> O <sub>3</sub>	0.0286±0.0015	--	--	--
AuBr <sub>3</sub>	0.0279±0.0014	--	--	--
Tl	--	0.0323	0.0298	0.0303
TlO <sub>2</sub>	0.0284±0.0014	--	--	--
Tl <sub>2</sub> O <sub>3</sub>	0.0290±0.0015	--	--	--
TlNO <sub>3</sub>	0.0277±0.0014	--	--	--
Tl <sub>2</sub> CO <sub>3</sub>	0.0282±0.0014	--	--	--

The differences can be explained by using the electronegativity value of elements and it can be reach to Pauling electronegativity values in Table 3 for elements included in chemical compounds.

Table 3. Pauling electronegativity values of elements

Element	Z	Pauling Electronegativity
C	6	2.55
N	7	3.04
O	8	3.44
Br	35	2.96
Pt	78	2.28
Au	79	2.54
Tl	81	1.62

From Table 3, it can be seen that oxygen atom is the most electronegative and it will cause maximum changes in the chemical compounds. When the Pt and Au compounds are examined, the maximum changes (37% and 35%) can be seen for oxidized compounds of Pt and Au. The brominated compounds of Pt and Au show lesser increment (32%) in the measured  $M_{\alpha}$  and  $M_{\beta}$  X-ray production cross-section values. The reason of these differences is the effective nuclear charge felt by outer N shell. The most electronegative atoms in the same chemical compound attract the outer shell electrons of neighbouring atom. In this case two situations are possible. First is the transferring of outermost electrons caused by the electronegativity differences between atoms in chemical compound and second is the polarizability of high atomic number atoms. First case increases the probability of X-ray production for atoms with lower electronegative

value. Since transferring of outer shell electrons from lower electronegative atom to higher increases the effective nuclear charge in lower electronegative element, the electronic levels will shift toward to internal levels. The inner shell electrons are more tightly bound than that of outer shells. The increment in the binding energy of electrons increases the probability of X-ray transitions. In the second case, the element with the highest electronegative value polarizes the high atomic number element even if the most electronegative element has smaller size. The polarized states shift to the outermost levels reducing the binding energy of electrons. The decreasing binding energy increases the non-radiative transition probability and so the reductions should be observed in the measured  $M_{\alpha}$  and  $M_{\beta}$  X-ray production cross-section values. But in this study, no reduction is observed.

The similar tendency can be seen for Tl compounds in Table 1 but an important point has been identified. First identified point is that, the measured parameters in Table 1 are not dependent on the oxidation state of Tl. Fig. 4 shows the  $M_{\alpha}$  and  $M_{\beta}$  X-ray production cross-section values for produced chemical compounds in this study. In this figure, the points in right side are belong to the Tl compounds and it can be seen that the change ratio of parameters are not related with the decreasing oxidation state which are +4, +3 +1 and +1 for  $TlO_2$ ,  $Tl_2O_3$ ,  $TlNO_3$  and  $Tl_2CO_3$  respectively. Second, the changes are lower for oxidized compounds of Tl than that of Au and Pt. And third, the percentage change ratios are the lowest for  $TlNO_3$  and  $Tl_2CO_3$  compounds even if two electronegative elements than Tl are included.

Fig. 5 shows the average M shell fluorescence yield of Pt, Au and Tl compounds. From the measurements, it is observed that the error bars are within the experimental error limits and so nothing can be said about the changes of M shell fluorescence yield measurements. The uncertainties in the measurements result from the non-uniform thickness ( $\leq 2\%$ ), counting statistics ( $\leq 3\%$ ),  $I_0G\epsilon$  factor ( $\leq 2\%$ ) and finally absorption coefficients at incident and emitted photon energies ( $\leq 3\%$ ). In this study the experimental error limit is determined as less than 7%.

The changing inside experimental error limit is due to the closeness of M shell in high atomic number elements. The innermost shells are attracted by nucleus and these

shells feel the most effective nuclear charge. And so, these electronic levels cannot be easily affected by the changes in electronic structure or number of valence electrons.

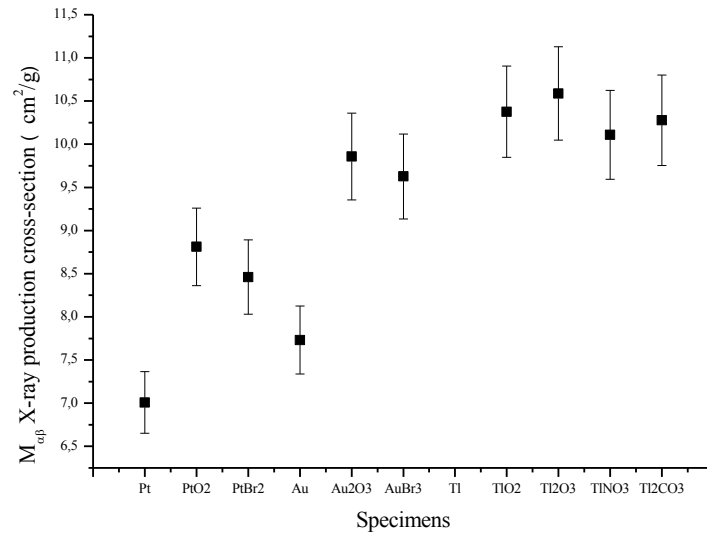


Figure 4. The changes of  $M_{\alpha\beta}$  X-ray production cross-section values

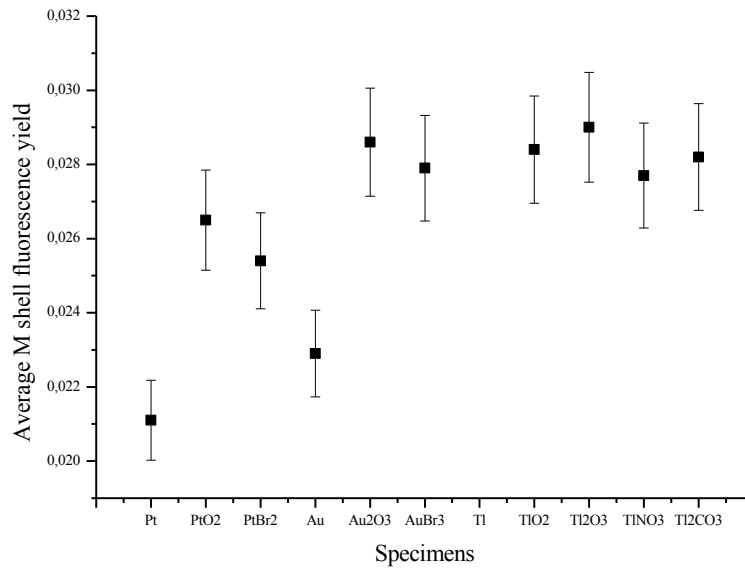


Figure 5. The average M shell fluorescence yield of compounds

#### 4. Conclusions

The measurements of M shell parameters in the concept of this study will shed light on the complex structure of M sub-shell and X-ray transitions from upper shells to this studied shell for different Au, Pt and Tl compounds even if the  $M_{\alpha}$  and  $M_{\beta}$  X-rays cannot be resolved from each other. And more X-ray parameters must be determined for pure elements, alloys or compounds for the theoretical investigations and for the designing of new, more sensitive and technological devices for quantitative analysis, radiation measurement and etc. More data will be helpful for the understanding of complex structure of electronic shell and quantum mechanical motion of electrons which obeys Heisenberg uncertainty principle.

The complexity structure of M sub-shell cause to fewer studies compared to the K and L shells. Since the oxygen is the most electronegative element, the biggest percentage changes are observed in  $M\alpha\beta$  X-ray production cross-section values for  $PtO_2$  and  $Au_2O_3$ . For the average M shell fluorescence yields, the values change inside experimental error limit since these sub-shells cannot easily be affected by the different number of electrons. Also, it is believed that these measurements will constitute fundamental data for the theoretical estimations of atomic structure calculations.

#### References

- [1] Aylikci, N.K., Aylikci, V., Kahoul, A., Tirasoglu, E., Karahan, I.H., Cengiz, E., *Effect of pH treatment on K-shell X-ray intensity ratios and K-shell X-ray production cross-sections in ZnCo alloys*, Physical Review A, 84, 042509, 2011.
- [2] Yang, Y., *Structural and dynamical properties of water adsorption on PtO<sub>2</sub>(001)*, RSC. Advances, 8, 15078-15086, 2018
- [3] Tanzer, K., Pelc, A., Huber, S.E., Smialek, M.A., Scheier, P., Probst, M., Denifl, S., *Low energy electron attachment to platinum (II) bromide*, International Journal of Mass Spectrometry, 365-366, 152-156, 2014.
- [4] Shi, H., Asahi, R., Stampfl, C., *Properties of the gold oxides Au<sub>2</sub>O<sub>3</sub> and Au<sub>2</sub>O: First principle investigation*, Physical Review B, 75, 205125, 2007.
- [5] Kwon, C.K., Kim, B.J., Lee, J.L., Kim, S.Y., *Effect of anions in Au complexes on doping and degradation of graphene*, Journal of Materials Chemistry C, 1, 2463-2469, 2013.

[6] Ertugrul, M., Sade, K., Erdogan, H., *Calculation of M x-ray production cross sections from 1–1500 keV in the atomic region  $70 \leq Z \leq 92$* , X-ray Spectrometry, 33, 136-145, 2004.

[7] Ertugrul, M., Tirasoglu, E., Kurucu, Y., Erzenoglu, S., Durak, R., Sahin, Y., *Measurement of M shell X-ray production cross-sections and fluorescence yields for the elements in the atomic range  $70 \leq Z \leq 92$  at 5.96 keV*, Nuclear Instruments and Methods in Physics Research Section B, 108, 18-22, 1996.

[8] Puri, S., Mehta, D., Chand, B., Singh, N., Mangal, P.C., Trehan, P.N., *M shell X-ray production cross sections and fluorescence yields for the elements with  $71 \leq Z \leq 92$  using 5.96 keV photons*, Nuclear Instruments and Methods in Physics Research Section B, 73, 319-323, 1993.

[9] Rao, D.V., Cesareo, R., Gigante, G.E., *Total M X-ray fluorescence cross sections and fluorescence yields for Pt, Au and Pb in the energy region  $5.47 \leq E \leq 9.36$  keV*, Nuclear Instruments and Methods in Physics Research Section B, 108, 227-232, 1996.

[10] Chauhan, Y., Kumar, A., Puri, S., *M shell X-ray production cross-sections for elements with  $67 \leq Z \leq 92$  at incident photon energies  $E_{M1} < E_{inc} \leq 150$  keV*, Atomic Data and Nuclear Data Tables, 95, 475-500, 2009.

[11] Kaur, G., Gupta, S., Tiwari, M.K., Mittal, R., *M sub-shell X-ray emission cross-section measurements for Pt, Au, Hg, Pb, Th and U at 8 and 10 keV synchrotron photons*, Nuclear Instruments and Methods in Physics Research Section B, 320, 37-45, 2014.

[12] Ozdemir, Y. *Differential and total M-shell X-ray production cross-sections of some selected elements between Au and U at 5.96 keV*, Nuclear Instruments and Methods in Physics Research Section B, 256, 581-585, 2007.

[13] Deghfel, B., Kahoul, A., Nekkab, M., *Hafnium to thorium M-shell X-ray production cross sections by proton impact*, Journal of Radiation Research and Applied Sciences, 7, 512-518, 2014.

[14] Sampaio, J.M., Guerra, M., Parente, F., Madeira, T.I., Indelicato, P., Santos, J.P., *Calculations of photo-induced X-ray production cross-sections in the energy range 1–150 keV and average fluorescence yields for Zn, Cd and Hg*, Atomic Data and Nuclear Data Tables, 111-112, 67-86, 2016.

[15] Mainardi, R.T., *On the angular dependence of differential and total M-shell X-ray production cross-sections*, Nuclear Instruments and Methods in Physics Research Section B, 267, 1989-1990, 2009.

[16] Kaya, N., Apaydin, G., Aylikci, V., Cengiz, E., Tirasoglu, E., *K shell, L shell–subshell and M shell–subshell photoeffect cross-sections in elements between Tb ( $Z = 65$ ) and U ( $Z = 92$ ) at 123.6 keV*, Radiation Physics and Chemistry, 77, 101-106, 2008.

[17] Sampaio, J.M., Madeira, T.I., Parente, F., Indelicato, P., Santos, J.P., Marques, J.P., *Relativistic calculations of M-shell photoionization and X-ray production cross-sections for Hg at 5.96 keV excitation energy*, Radiation Physics and Chemistry, 107, 36-39, 2015.

[18] Rao, D.V., Cesareo, R., Gigante, G.E., *Average M-Shell fluorescence yields for Pt, Au and Pb*, Radiation Physics and Chemistry, 49, 503-504, 1997.

[19] Ozdemir, Y., Durak, R., Esmer, K., Ertugrul, M., *Measurement of angular dependence from L3-subshell to M-shell vacancy transfer probabilities for the elements in the atomic region  $71 \leq Z \leq 78$* , Journal of Quantitative Spectroscopy and Radiative Transfer, 90, 161-168, 2005.

[20] Kaur, G., Mittal, R., *M sub-shell fluorescence and Coster-Kronig yield data generation for elements,  $57 \leq Z \leq 90$  (computer code 'MFCKYLD')*, Journal of Quantitative Spectroscopy and Radiative Transfer, 133, 489-503, 2014.

[21] Sampaio, J.M., Madeira, T.I., Guerra, M., Parente, F., Indelicato, P., Santos, J.P., Marques, J.P., *Relativistic calculations of K-, L- and M-shell X-ray production cross-sections by electron impact for Ne, Ar, Kr, Xe, Rn and Uuo*, Journal of Quantitative Spectroscopy and Radiative Transfer, 182, 87-93, 2016.

[22] Bansal, H., Tiwari, M.K., Mittal, R., *M sub-shell X-ray fluorescence cross-section measurements for six elements in the range  $Z = 78-92$  at tuned synchrotron photon energies 5, 7 and 9 keV*, Journal of Quantitative Spectroscopy and Radiative Transfer, 204, 232-241, 2018.

[23] Ozdemir, Y., Durak, R., *Angular dependence from L3-subshell to M-shell vacancy transfer probabilities for heavy elements using EDXRF technique*, Annals of Nuclear Energy, 35, 1335-1339, 2008.

[24] Kainth, H.S., Singh, R., Singh, G., Mehta, D., *Chemical shift in  $L\alpha$ ,  $L\beta_1$ ,  $L\beta_{3,4}$ ,  $L\beta_{2,15}$ ,  $L\gamma_1$  and  $L\gamma_{2,3}$  emission lines of  $47Ag$ ,  $48Cd$  and  $50Sn$  compounds*, Nuclear Instruments and Methods in Physics Research Section B, 414, 84-98, 2018.

[25] Wang, X., Zhao, Y., Cheng, R., Zhou, X., Xu, G., Sun, Y., Lei, Y., Wang, Y., Ren, J., Yu, Y., Li, Y., Zhang, X., Li, Y., Liang, C., Xiao, G., *Multiple ionization effects in M X-ray emission induced by heavy ions*, Physics Letters A, 376, 1197-1200, 2012.

[26] Pajek, M., Banas, D., Jablonski, L., Mukoyama, T., *Electronic wave function and binding effects in M-shell ionization of gold by protons*, Nuclear Instruments and Methods in Physics Research Section B, 417, 15-18, 2018.

[27] Cengiz E., Aylikci, V., Kaya, N., Apaydin, G., Tirasoglu, E., *Chemical effects on K and L shell production cross-sections and transfer probabilities in Nb compounds*, Journal of Radioanalytical and Nuclear Chemistry, 278, 89-96, 2008.

- [28] Apaydin, G., Aylikci, V., Cengiz E., Saydam, M., Kup, N., Tirasoglu, E., *Analysis of metal contents of Seaweed (Ulva lactuca) from Istanbul, Turkey by EDXRF*, Turkish Journal of Fisheries and Aquatic Sciences, 10, 215-220, 2010.
- [29] Aylikci, V., Cengiz E., Apaydin, G., Unver, Y., Sancak, K., Tirasoglu, E., *Influence of functional group effect on the K-shell X-ray production cross-sections and average fluorescence yields of sulphur in 1,2,4-triazol-5-one compounds containing thiophene*, Chemical Physics Letters, 461, 332-337, 2008.
- [30] Berger, M.J., Hubbell, J.H., XCOM: Photon cross-sections on a personal computer (version 1.2), NBSIR85-3597, National Bureau of Standards, Gaithersburg, MD, USA, for version 3.1, 1999.
- [31] Storm, E., Israel, I., *Photon Cross Sections from 1 keV to 100 MeV for Elements Z=1 to Z=100*, Nuclear Data Tables, A7, 565-681, 1970.
- [32] Scofield, J.H., *Theoretical photoionization cross sections from 1 to 1500 keV*, California Univ., Livermore. Lawrence Livermore Lab., 1973.
- [33] McGuire, E.J., *Atomic M-shell Coster-Kronig, Auger, radiative and fluorescence yields for Ca-Th*, Physical Review A, 5, 1043-1047, 1972.
- [34] Kucukonder, A., Sogut, O., Dozen, C., Durdu, B.G., *Measurement of M-shell X-ray production cross-sections for the element  $73 \leq Z \leq 83$  using 5.96 keV photons*, The European Physical Journal D, 46, 37-39, 2008.
- [35] Durak, R., Ozdemir, Y., *Photon-induced M-shell X-ray production cross-sections and fluorescence yields in heavy elements at 5.96 keV*, Spectrochimica Acta Part B: Atomic Spectroscopy, 56, 455-464, 2001.
- [36] Chen, M.H., Crasemann, B., *Relativistic M-shell radiationless transitions*, Physical Review A, 21, 449-453, 1980.
- [37] Oz, E., Erdogan, H., Ertugrul, M., *Calculation of average M-shell fluorescence yields for elements with  $29 \leq Z \leq 100$* , X Ray Spectrometry, 28, 198-202, 1999.